https://doi.org/10.5194/bg-2023-134
Preprint. Discussion started: 17 August 2023

Biogeosciences Discussions Open Access EGU

Quantification of allochthonous and autochthonous organic carbon in large and shallow Lake Wuliangsu based on distribution patterns and $\delta^{13}C$ signatures of *n*-alkanes

Qingfeng Zhao[1], Aifeng Zhou[2], Yuxin He[1*]

[1] Organic Geochemistry Unit, Key Laboratory of Geoscience Big Data and Deep Resource of Zhejiang Province, School of Earth Sciences, Zhejiang University, Hangzhou, 310058, China

[2] Key Laboratory of Western China's Environmental Systems (Ministry of Education), College of Earth and Environmental Sciences, Lanzhou University, Lanzhou, 730000, China

Correspondence to: Yuxin He (yxhe@zju.edu.cn)

Abstract:

Identification and quantification of allochthonous and autochthonous organic carbon (OC) are crucial for the interpretation of burial behaviors of sedimentary OC of shallow lakes under anthropogenic interferences. In this study, we analyzed distribution patterns and $\delta^{13}C$ signatures of mid- and long-chain *n*-alkanes on various types of surface samples from a typically large and shallow Lake Wuliangsu in the Hetao Irrigation District. The results indicate that *n*-alkanes among submerged macrophytes, emergent plants, and riverine soil show unique distribution patterns and $\delta^{13}C$ signatures, supporting the practicability of quantification on OC of these sources by end-member mixing models. Introducing the $\delta^{13}C$ values of *n*-alkanes into the end-member mixing models could effectively reduce the potential error derived from end-member determination on *n*-alkane distribution patterns and OC degradation. The model results suggest that the riverine sourced OC from the main channel to Lake Wuliangsu has settled down during the southward migration process. Therefore, Lake Wuliangsu serves as an important trap and sink for the allochthonous OC from the Upper Yellow River Reaches. The model results also show a predominate contribution from the autochthonous OC to Lake Wuliangsu (mostly >85%), with open-water areas dominated by submerged macrophytes and the rest of areas by emergent plants, largely modulated by water transparency, water depth, and nutrient concentrations. Together with previously published tetraether results, we further proposed that areas dominated by submerged macrophytes might be more favorable for heterotrophic anaerobic bacteria and methanogenic archaea, largely due to active recycling processes for the labile OC derived from submerged macrophytes.

Keywords: Allochthonous *vs*. autochthonous OC, Lake Wuliangsu, *n*-alkanes, distribution patterns, $\delta^{13}C$ values, end-member mixing model

1. Introduction

Shallow lakes (max water depth < 4 m), accounting for the largest area of lakes globally (Downing et al. 2006; Verpoorter et al., 2014), are very sensitive to climatic variations and land use and land cover (LULC) change (Sivakumar et al., 2005;

https://doi.org/10.5194/bg-2023-134
Preprint. Discussion started: 17 August 2023

Harpenslager et al., 2022). As the largest lake ecosystem in the reaches of the Yellow River, Lake Wuliangsu is a typical semi-arid shallow lake that has undergone strong eutrophication and paludification due to rapid industrialization and urbanization over the last decades. For instance, substantial nutrients input from agricultural and industrial activities have triggered eutrophication of this lake, resulting in stronger organic carbon (OC) burial and severer damage to the lake ecosystem (He et al., 2015, 2022; Shen et al., 2016; Sun et al., 2019). Meanwhile, autochthonous bioproductivity accumulation, allochthonous detritus siltation, and water loss together have resulted in intensive paludification of Lake Wuliangsu (Duan et al., 2005; Lü et al., 2008; He et al., 2015). Therefore, knowledge of OC burial behavior of Lake Wuliangsu under anthropogenic interferences would provide an important reference for sustainable management practices of shallow lakes regionally and globally.

Generally, allochthonous OC (terrestrial input) and autochthonous OC (primary bioproductivity) in shallow lake systems show different characteristics on perspectives of source and sink behaviors (Alahuhta et al., 2014). On one hand, Lake Wuliangsu receives allochthonous materials from the surrounding catchment through local precipitation and discharge, and the Upper Yellow River Reaches via the western inlet channels (Wu et al., 2013). On the other hand, the *in-situ* bioproductivity of Lake Wuliangsu is mainly contributed by submerged macrophytes and emergent plants (Sun et al., 2006; Tian et al., 2011; Fu et al., 2013; Zhang. 2017; Du et al., 2022; Ni et al., 2022), which show different ecological functions and OC burial characteristics (Botrel and Maranger, 2023). The stems and leaves of submerged macrophytes can adsorb heavy metals from water, and fix pollutants through their roots to improve the quality of lake water bodies (Zhu et al., 2018). Also, the outspread of submerged macrophytes would increase the carbon dioxide (CO_2) and methane (CH_4) release through the methanogenic decomposition of plant exudations and debris (Li et al., 2019; He et al., 2023). Alternatively, emergent plants have a greater capacity for nutrient accumulation, and could significantly impact the biodiversity of macroinvertebrates within the vegetated area (Zhao et al., 2012). Emergent plants also accelerate the paludification of shallow lakes, largely due to their stronger evapotranspiration and faster siltation (Zhou and Zhou, 2009). Therefore, identification and quantification of OC from these sources would be very crucial to the interpretation of burial and decomposing behaviors of sedimentary OC in shallow lakes.

Over the past decades, many studies have attempted to evaluate the relative contributions of allochthonous and autochthonous OC to Lake Wuliangsu. For instance, previous studies have suggested a major contribution of autochthonous OC to Lake Wuliangsu, as evidenced by similar spatial distribution between the autochthonous biomass and the sedimentary TOC values (Sun et al., 2006; Tian et al., 2011; Fu et al., 2013). Also, *in-situ* biomasses of both submerged macrophytes and emergent plants have been directly evaluated by remote sensing techniques and on-site investigations (Zhang, 2017; Du et al., 2022; Ni et al., 2022). The results have shown that half of the lake area is covered by emergent plants (known as vegetation-covered areas), while the other half is covered by submerged macrophytes and clear water (known as open-water areas, Zhang, 2017). Alternatively, the amount of phytoplankton is relatively lower compared to the widespread emergent plants and submerged macrophytes (Ni et al., 2022). In terms of seasonality, the biomass of submerged macrophytes is higher in September than in July (Du et al., 2022), while the biomass of emergent plants is higher in summer (June to August) than in

https://doi.org/10.5194/bg-2023-134
Preprint. Discussion started: 17 August 2023

winter (January), largely due to artificial harvesting (Yang et al., 2009). Unfortunately, these studies have hardly quantified the individual OC burial behaviors of both submerged macrophytes and emergent plants, let alone their comparison with the allochthonous OC, asking for new methods to further evaluate the relative contributions of different OC sources to Lake Wuliangsu.

n-Alkanes have been proven to be useful in differentiating OC sources in lake system (Ficken et al., 2000; Castañeda and Schouten, 2011). Generally, *n*-alkanes of both terrestrial vascular plants and emergent plants are characterized by the predominance of long-chain homologues (*n*-C_{27}, *n*-C_{29}, and *n*-C_{31}). Alternatively, submerged plants mainly display a high abundance of mid-chain homologues (*n*-C_{23} and *n*-C_{25}), distinctive from both terrestrial and emergent plants (Ficken et al., 2000; Aichner et al., 2010; Liu and Liu, 2016; Andrae et al., 2020). *n*-Alkanes have been successfully applied into Lake Wuliangsu on a sedimentary core for the reconstruction of ecological dynamics since the Industrial Era (He et al., 2015). However, without proper identification of *n*-alkane from modern samples as end-members, applications of *n*-alkanes might be slightly hindered by overlaps in *n*-alkane compounds from various OC sources (Liu and Liu, 2016; Dion-kirschner et al., 2020). Firstly, the contributions of long-chain *n*-alkanes from submerged macrophytes (Liu et al. 2018), as well as mid-chain *n*-alkanes from emergent plants and terrestrial plants (Sinninghe Damsté et al., 2011) should be taken into consideration. Secondly, emergent plants and terrestrial vascular plants both yield similar long-chain *n*-alkane predominance, usually resulting in inevitable difficulty in separating both sources in shallow lakes (Liu and Liu, 2016). Thirdly, subsequent degradation of *n*-alkanes during and after deposition might potentially increase the average carbon chain length, bringing uncertainties into the application of *n*-alkane distribution patterns in differentiating OC sources (Van Beilen et al., 2003; Wang et al., 2019).

Compound specific $\delta^{13}C$ values of *n*-alkanes serve as another independent tool for identification and quantification of allochthonous and autochthonous OC (Sinninghe Damsté et al., 2011; Holtvoeth et al., 2019; Struck et al., 2019), considering large $\delta^{13}C$ differences in *n*-alkanes among different sources (Freeman et al., 1994) and little isotopic fractionation during photo-oxidation and microbial degradation of *n*-alkanes (Ahad et al., 2011; Hyun et al., 2017). For autochthonous OC, submerged macrophytes show relatively positive $\delta^{13}C$ values of *n*-alkanes (e.g., –26.3‰ to –13.3‰, Aichner et al., 2010), while emergent plants show much more negative $\delta^{13}C$ values in *n*-alkanes (e.g., –35.3‰ to –28.7‰, Duan et al., 2011; Ho et al., 2015). The $\delta^{13}C$ values of soil OC are dependent on the natures of photosynthesis pathways of the sourced terrestrial plants (C_3 *vs.* C_4, –39.0‰ to –32.0‰ *vs.* –25.0‰ to –18.0‰, Collister et al., 1994). A previous study on a sedimentary core in Lake Wuliangsu suggested different photosynthesis pathways between mid- and long-chain *n*-alkanes, considering that $\delta^{13}C$ values of mid-chain *n*-alkanes were up to 7–9‰ more positive than those of long-chain ones in the same sample (He et al., 2015). They also found that $\delta^{13}C$ values are more depleted in both mid- and long-chain *n*-alkanes in Lake Wuliangsu after the 1990s than those during the 1950s–1970s, tentatively signaling a shift in the OC sources upon time sequence. Accordingly, with the assistance of compound-specific $\delta^{13}C$ analysis, sources of *n*-alkanes in Lake Wuliangsu can be further elucidated.

https://doi.org/10.5194/bg-2023-134
Preprint. Discussion started: 17 August 2023

In this study, we analyzed the distribution patterns and $\delta^{13}C$ values of mid- and long-chain *n*-alkanes from modern aquatic plants and surface sediments collected from the large and shallow Lake Wuliangsu. We aim to identify the distribution patterns and $\delta^{13}C$ characteristics of *n*-alkanes from major contributors to the sedimentary OC of Lake Wuliangsu, and develop quantitative/semi-quantitative methods to calculate the relative contributions to sediments from different OC sources based on the end-member mixing models. We also discussed whether introducing the $\delta^{13}C$ values of *n*-alkanes into the end-member mixing models could effectively reduce the potential uncertainty. With the new end-member mixing models, we probed the spatial pattern and the controlling factors of allochthonous and autochthonous OC of Lake Wuliangsu under anthropogenic interferences, which would provide an important reference for sustainable management practices of shallow lakes regionally and globally.

2. Materials and methods

2.1 Geographical background

Lake Wuliangsu (40°47′–41°03′N,108°43′–108°57′E) located in the Upper Yellow River Reaches, China (Figure. 1), covers a surface area of 371 km^2. It is an alkaline (pH of 9.04) and fresh lake (salinity of 2.48 g/L, Ma et al., 2013), with a mean depth of 1–1.5 m and a maximum depth of 2.5–3.0 m (Song et al., 2019). According to the meteorological data from Urad Qianqi station, mean annual air temperature, precipitation, and potential evapotranspiration are 7.5 °C, 225, and 2140 mm, respectively (data from http://www.ntsg.umt.edu), resulting in strong water loss (Sun et al., 2013). Lake Wuliangsu is surrounded by Lang Mountains to the north, Wula Mountain to the east, and the Yellow River floodplain to the west and the south (Wu et al., 2013). It mainly receives discharge from the Hetao Irrigation District via six irrigation channels from the west bank, with the main channel (also known as the Wujia River) contributing ~90% of the total materials (Yang et al., 2019). Annual agricultural nutrient input into Lake Wuliangsu from the surrounding farm areas is ~65.75 t/yr (Ni et al., 2022). Dense emergent plants and submerged macrophytes are widely distributed across the Lake Wuliangsu under hypereutrophic conditions. Almost half of areas is covered with emergent plants (e.g., *Phragmites communis*), whereas submerged macrophytes (e.g., *Potamogeton pectinatus*) become the predominant aquatic vegetation in the open-water area (Lü et al., 2008). Aquatic litters from submerged macrophytes and emergent plants quickly accumulated at the lake bottom at the rate of ~9–13 mm/yr, leading to server paludification for Lake Wuliangsu (Yu et al., 2007).

2.2 Sample collection

In July 2019, lake surface sediment samples (< 3 cm) were collected from 14 different locations within Lake Wuliangsu (sites S1–S14, Figure. 1). For the 14 surface sediments, samples S3, S11, S12, S13, and S14 were collected in areas mainly covered by submerged macrophytes (open-water area), while samples S1, S2, S4, S5, S6, S7, S8, S9, and S10 were in areas mainly covered by emergent plants (vegetated area). Seven lake shore surface sediments (<3 cm) around the lake (sites SS1–

https://doi.org/10.5194/bg-2023-134
Preprint. Discussion started: 17 August 2023

SS7, Figure. 1) were also collected. One riverine surface sediment (<5 cm) was collected at the end section of the main irrigation channel (site WJ, Figure.1) to track riverine OC input. Furthermore, aquatic plants of *Phragmites communis* and *Potamogeton pectinatus* were collected for the OC source appointment of emergent plants and submerged macrophytes. All samples were preserved in a –20 ºC refrigerator immediately after being collected in the field and were freeze-dried once taken back to the laboratory.

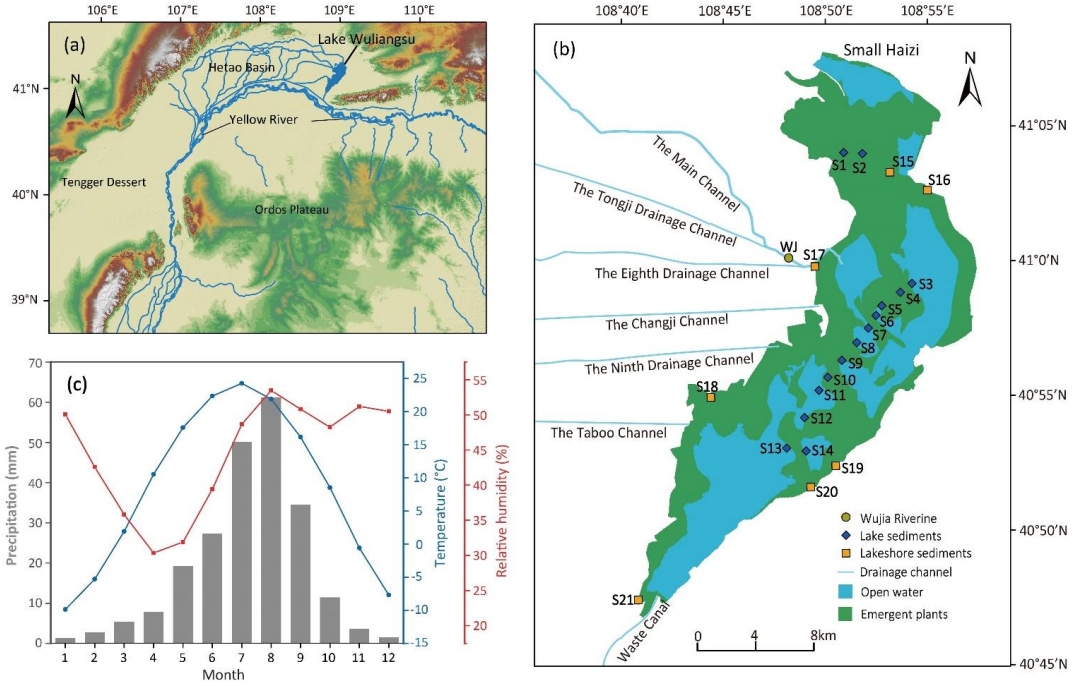

Figure 1. Location and setting. (a) Map showing the location of study site Lake Wuliangsu (blue area) in the northern Chinese Loess Plateau. (b) the geophysical showing the hydrological condition and sample sites, the dark blue rhombus and orange square indicate the sampling sites within the lake and lakeshore, respectively. And the green and blue regions are *Phragmites australis* growth zones and open-water zones, (c) mean monthly precipitation, temperature, and relative humidity (1981-2015) from Urad Qianqi station, China (data from China Meteorological Administration https://data.cma.cn/), which is closed to Lake Wuliangsu.

2.3 Bulk organic carbon analyses

Samples for total organic carbon (TOC) analysis were treated with 6N HCl at 60 ºC, heated for 2 h to remove carbonates, and subsequently rinsed with deionized water to neutral. The carbonates-free samples were then dried at 40 ºC and further analyzed for TOC contents on a Euro Vector EA 3000 Elemental Analyzer. The standard samples were analyzed between every six samples, and the 1 σ precision of replicate analysis is ±0.02% for TOC analysis.

2.4 *n*-Alkane analysis

All the freeze-dried sample (~10 g sediments and ~1 g plant samples) were extracted ultrasonically with the solves of

https://doi.org/10.5194/bg-2023-134
Preprint. Discussion started: 17 August 2023

dichloromethane/methanol (9: 1, v/v). After drying with a gentle N_2 stream, the extracted lipids were then saponified with 6% KOH in methanol and further extracted with *n*-hexane to get the neutral fraction. The apolar fraction containing *n*-alkanes was further obtained from the neutral fraction by silica gel liquid chromatography using *n*-hexane as eluent. Quantification was obtained using an Agilent 7890A gas chromatograph (GC) equipped with a flame ionization detector (FID). The GC was equipped with a DB-1MS capillary column (60 m×0.32 mm ×0.25 μm film thickness). Each sample was injected in splitless mode, with a GC inlet temperature of 295 ºC and a flow rate of 1.0 mL/min. The oven temperature was initially 60 ºC (held for 2 min), then increased to 300 ºC at 4 ºC /min, and finally held for 30 min. Individual *n*-alkane peak areas were compared with external standards (*n*-tetracosane-d_{50}) with known concentrations to calculate the concentrations of *n*-alkanes. Analytical uncertainty for concentrations of *n*-alkanes would be less than 5%, and the distribution pattern of the *n*-alkanes are only slightly impacted by the analytical uncertainty. *n*-Alkane-based P_{aq} (proportion of aquatic plants) and CPI (carbon preference index) proxies were calculated using the following equations provided in the Supplementary Material.

2.5 Compound-specific $\delta^{13}C$ analysis

The neutral fraction containing *n*-alkanes was further separated into *n*-alkanes and branched/cyclic alkanes by urea adduction. Compound-specific $\delta^{13}C$ values of *n*-alkanes of lake sediments were measured in Thermo-Fisher Scientific Trace GC coupled with a MAT 253 isotope ratio mass spectrometry (IRMS). The GC was also equipped with a DB-1MS capillary column (60 m×0.32 mm×0.25 μm film thickness). Helium with a flow rate of 1.4 mL/min was used as carrier gas. The GC oven temperature was initiated at 80 °C (held for 2 min), then increased to 300 ºC by 3 ºC/min, and finally held for 30 min. An external standard consisting of a mixture of *n*-C_{16} to *n*-C_{30} alkanes with known isotopic values (B4, Indiana University) was measured routinely to ensure the data quality. The carbon isotope ratios are expressed in ‰ relative to the V-PDB standard, and the 1 σ precision of the replicate measurement on standard samples was < ±0.3‰.

3. Results

3.1 TOC values

The averaged TOC values for lake sediments, lakeshore sediments, and riverine sediment are 3.30% (0.71%–7.19%, n=14), 0.78% (0.28%–1.30%, n=7), and 0.20%, respectively (Figure. 2a). Relatively higher TOC values in the lake sediments than those in the lakeshore and riverine sediments suggest an additional supply of autochthonous materials of higher TOC values (33.73% and 37.08% for submerged macrophytes and emergent plants). For the lake sediments, the TOC value was the highest in the central section of the lake (site S12, 7.19%) and the lowest near the main channel (site S4, 0.71%). Moreover, the TOC values of samples at the open-water area are slightly higher than those in the shallower vegetated area (avg. 5.53% *vs.* 3.02%). Therefore, the sedimentary TOC values might be impacted by both the dilution of the terrestrial detritus and the *in-situ* ecological conditions.

https://doi.org/10.5194/bg-2023-134
Preprint. Discussion started: 17 August 2023

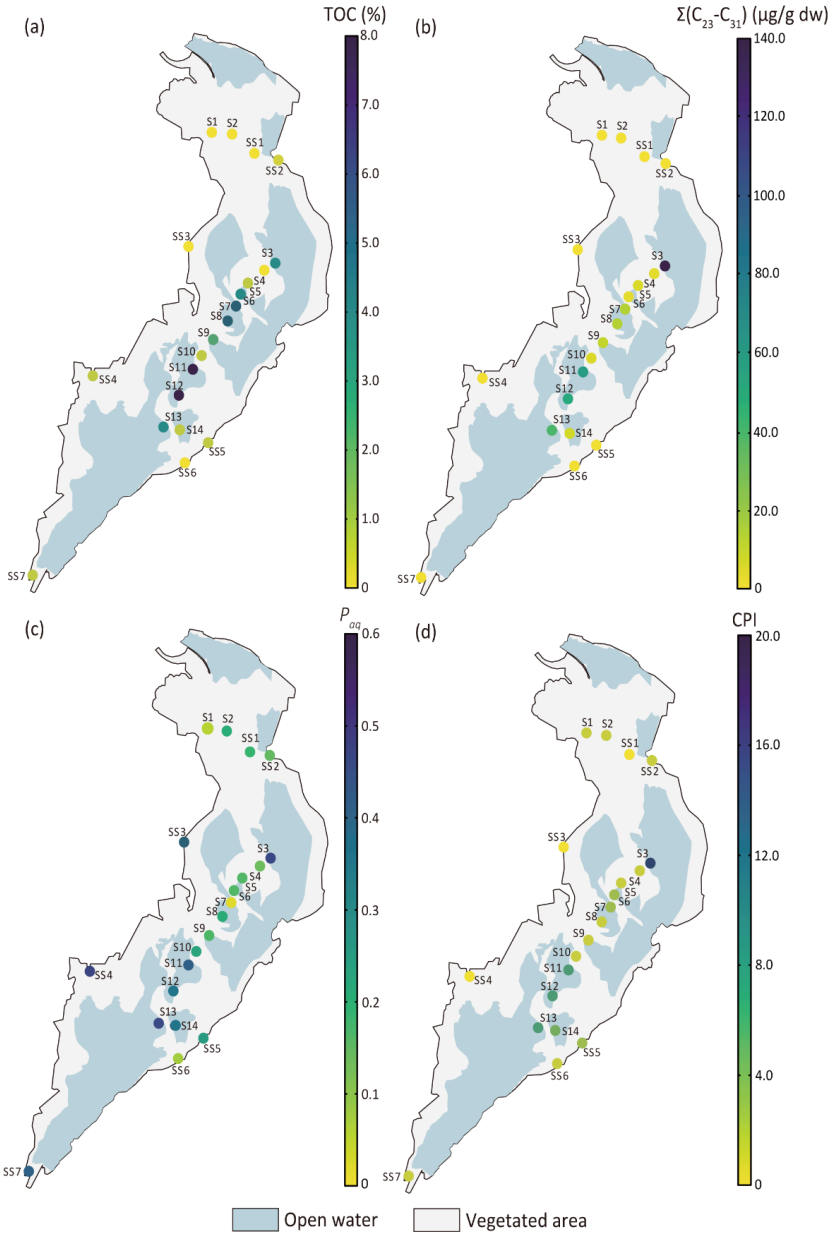

Figure 2. Spatial distribution of (a) TOC values, (b) concentrations of odd-chain *n*-C_{23} to *n*-C_{31} alkanes, (c) P_{aq} values, and (d) CPI values of lake and lakeshore sediments in Lake Wuliangsu.

3.2 Concentrations of *n*-alkanes

Total concentrations of *n*-C_{23} to *n*-C_{31} alkanes in lake sediments show strong variations, ranging from 0.62 μg/g to 137.05 μg/g (Figure. 2b, Supplementary Table S1). The lowest concentrations were observed in sediments in the northern vegetated area (sites S1 and S2), whereas the highest concentration were in the open-water area (sites S3 and S11, Figure. 2b).

https://doi.org/10.5194/bg-2023-134
Preprint. Discussion started: 17 August 2023

Considering that the total concentrations of *n*-C_{23} to *n*-C_{31} alkanes from submerged macrophytes and emergent plants are 132.75 μg/g (n=2) and 67.29 μg/g, respectively, sediments with *n*-alkane concentrations higher than 67.29 μg/g (i.e., sample S3) should be strongly contributed by submerged macrophytes instead of emergent plants. The total *n*-alkane concentration of the riverine sediment is 2.84 μg/g, much lower than those from submerged macrophytes and emergent plants. The total concentrations of *n*-C_{23} to *n*-C_{31} alkanes from the lakeshore sediments range from 0.79 μg/g to 3.54 μg/g, which are close to the lower end of lake sediments and the riverine sediment. The highest concentrations in lakeshore sediments were observed in the northeastern area (site SS2), whereas the lowest concentrations at the southeastern area (site SS5).

There was a significant positive correlation between TOC values and the concentrations of *n*-C_{23} to *n*-C_{31} alkanes among all sediments except for sample S3 (r^2=0.74, n=20, $p < 0.01$, Supplementary Figure S1). Such significant positive correlation also exists for all the individual alkane compound (r^2=0.65, 0.66, 0.71, 0.81, 0.85 for *n*-C_{23}, *n*-C_{25}, *n*-C_{27}, *n*-C_{29}, and *n*-C_{31}, respectively, n=20, $p < 0.01$). Considering that sample S3 contains a much higher *n*-alkane concentration, which is close to those of submerged macrophytes, we suggested that this sample might be largely influenced by pure supply from submerged macrophytes, and thus showed its unique correlation with TOC. Therefore, *n*-alkanes are still representative for most of sedimentary OC in Lake Wuliangsu.

3.3 Distribution patterns of *n*-alkanes

n-Alkanes of aquatic plants and surface sediments range from *n*-C_{17} to *n*-C_{31}, but show different distribution patterns in terms of mid- to long-chain compounds (Figure. 3a–c). For instance, submerged macrophytes were basically dominated by *n*-C_{23} and *n*-C_{25}, whereas emergent plants show the predominance of *n*-C_{27} and *n*-C_{29} components and trace occurrence of *n*-C_{31} alkane. Such *n*-alkane distribution patterns are similar to aquatic plants collected from lakes in Qinghai-Tibet Plateau (Aichner et al., 2010; Liu et al., 2015; Liu and Liu, 2016) and lower reaches of the Yangtze River (Yu et al., 2021). *n*-Alkanes of the riverine sediment (sample WJ) show a predominance of the *n*-C_{29} and *n*-C_{31} alkanes with low odd-chain predominance, slightly different from those of the emergent plants (Figure. 3). Accordingly, the P_{aq} values, the proxy evaluating the relative contributions of *n*-alkanes from aquatic plants (Ficken et al., 2000), are highest in submerged macrophyte (0.82), moderate in emergent plant (0.43) and lowest in riverine soil (0.21). The CPI values describing the odd-over-even predominance (Eglinton and Hamilton, 1967) are also highest in submerged macrophytes (18.02), moderate in emergent plants (10.24), and lowest in riverine soil (6.03, Figure. 2).

The distribution pattern of *n*-alkanes in lake sediments and lakeshore sediments show mixing signatures from submerged macrophytes, emergent plants, and riverine soil (Figure. 3d–f). Most of the sediments are characterized by *n*-C_{29} alkane as main peak, except for samples collected from sites S3 and SS4 characterized by *n*-C_{25} alkane as main peak. In lake sediments, the P_{aq} values range from 0.21 to 0.51, with higher values in samples located at both the northern (site S3) and the southern (site S13) open-water areas and lower values in samples located at the lake center (site S6, Figure. 2c). The CPI values range

https://doi.org/10.5194/bg-2023-134
Preprint. Discussion started: 17 August 2023

from 5.79 to 19.18, and show a strong correlation with the P_{aq} values (r^2=0.84, n=14, $p < 0.01$). The relatively high CPI values were observed at the southern (sites S11, S12, and S13) and the northern (site S3) open-water areas, whereas the lowest values were roughly at the lake center (site 10, Figure. 2d). In terms of lakeshore sediments, sample SS4 is characterized by relatively higher concentrations of *n*-C_{24} alkane, highest P_{aq} value (0.51) and lower CPI value (2.83). Together with the carbon isotopic evidence (Supplementary Table S1), we suspected that this sample might be contaminated by artificial products containing *n*-C_{23}, *n*-C_{24}, and *n*-C_{25} alkanes, and thus excluded this sample from any further discussion and evaluation. For the rest of the lakeshore sediments, the P_{aq} values and the CPI values range from 0.25 to 0.47 and from 3.62 to 7.26, respectively. The highest P_{aq} value was observed in the southern open-water area close to outlet channel (0.47, site SS7) and the lowest value was in the southeast far from the open-water area (0.25, site SS6). The highest CPI value was observed in the southeast far from the open-water area (7.26, site SS5), and the lowest value was close to the main inlet channel (3.62, site SS3). Different from the lake surface sediments, the CPI values of lakeshore sediments show weak but negative correlation with the P_{aq} values (r^2=0.10, n=6), tentatively suggesting that the even-chain *n*-alkanes of lakeshore sediments might be contaminated by oil contamination to some extent.

3.4 $\delta^{13}C$ signatures of *n*-alkanes

The $\delta^{13}C$ values of mid-and long-chain odd *n*-alkanes (*n*-C_{23}, *n*-C_{25}, *n*-C_{27}, *n*-C_{29}, and *n*-C_{31}) ranged from –36.6‰ to –24.1‰ (Figure. 3). Submerged macrophytes exhibited the most ^{13}C-enriched *n*-alkanes (–26.2‰ to –24.1‰), while *n*-alkanes from emergent plants were more depleted in ^{13}C values (–36.6‰ to –34.0‰), *n*-alkanes in riverine sediment show intermediate values (–33.1‰ to –30.7‰). The $\delta^{13}C$ values for mid- and long-chain *n*-alkanes of lake sediments range from –34.84‰ to –23.98‰ (Supplementary Table S1). In all sediments but sample S1, $\delta^{13}C$ values of *n*-alkanes show decreasing trend along with carbon length from *n*-C_{25} to *n*-C_{31}. $\delta^{13}C$ values of both mid- and long-chain *n*-alkanes in sediments at the open-water area (sites S3, S11, S12, S13, and S14) are more positive than those in other samples (Supplementary Table S1). In terms of lakeshore sediments, $\delta^{13}C$ values for mid- and long-chain *n*-alkanes ranged from –36.5‰ to –26.0‰. $\delta^{13}C$ values of *n*-alkanes show decreasing trend along with carbon length in samples SS1, SS3, SS5, and SS6. While *n*-C_{23} and *n*-C_{25} in SS4 were relatively depleted in ^{13}C (–34.4% to –34.3%), further supplementary the contamination by artificial products. The $\delta^{13}C$ values for *n*-C_{31} were the most positive in samples SS2 and SS7, tentatively suggesting more contribution of submerged macrophytes in single carbon at two sites.

https://doi.org/10.5194/bg-2023-134
Preprint. Discussion started: 17 August 2023

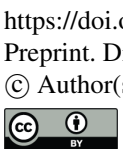

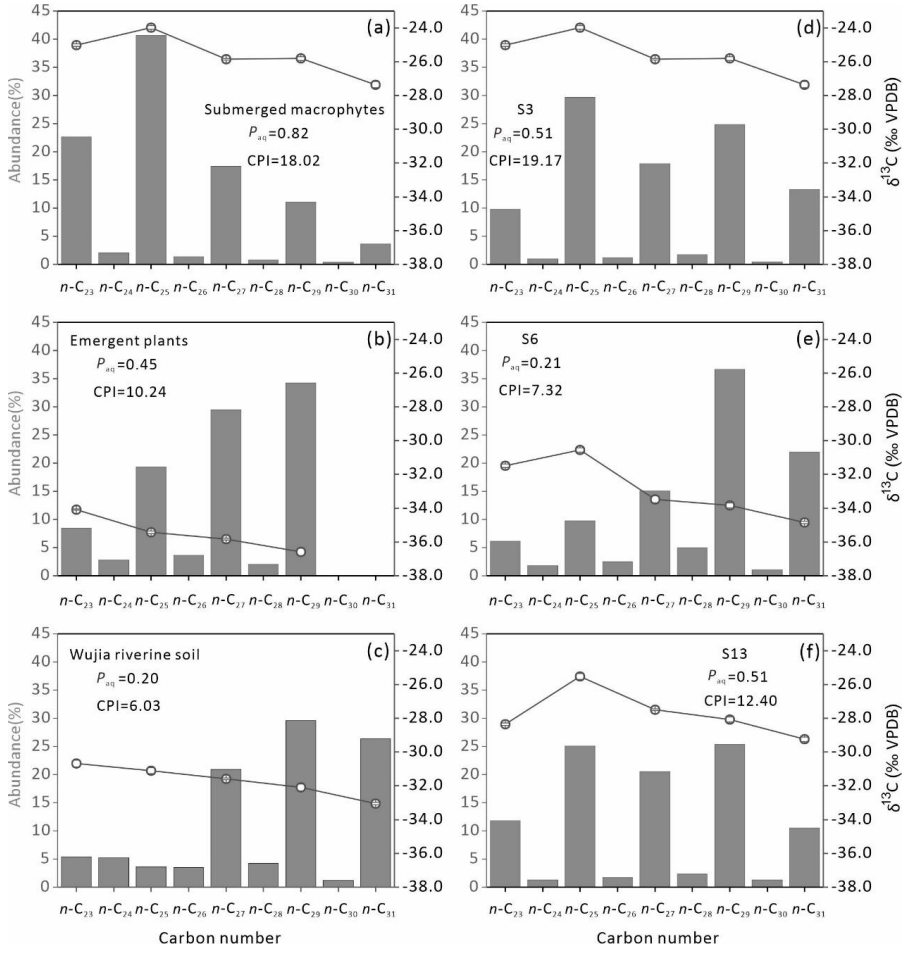

Figure 3. Bar plots and corresponding line graphs showing the distribution of the mid- and long-chain *n*-alkanes (relative abundance, left axis) and their stable carbon isotopic composition (right axis), for six representative sediments from the Lake Wuliangsu, including (a) submerged macrophytes (b) emergent plants (c) riverine soil (d) S3 (e) S6 (f) S13.

4. Discussion

4.1 Different *n*-alkane characteristics among various OC sources of Lake Wuliangsu

In Lake Wuliangsu, allochthonous and autochthonous OC showed distinct distribution patterns and $\delta^{13}C$ values of mid- and long-chain *n*-alkanes (Figure. 3). Generally, submerged macrophytes were characterized by a predominance of *n*-C_{23} and *n*-C_{25} alkanes and low concentrations of even-numbered chain *n*-alkanes, resulting in higher P_{aq} (0.82) and CPI (18.02) values. The $\delta^{13}C$ values of *n*-alkanes in submerged macrophytes were more ^{13}C-enriched (–24.1‰ to –26.2‰), consistent with other studies on shallow lakes globally (e.g., Aichner et al., 2010; Liu et al., 2015; Liu and Liu, 2016; Yu et al., 2021). Similar to emergent plants collected in many Chinese shallow lakes (e.g., Lake Shijiu, Lake Yangcheng, Lake Xihu, and Lake Hong,

https://doi.org/10.5194/bg-2023-134
Preprint. Discussion started: 17 August 2023

Duan and He, 2011; Ho et al., 2015; Yu et al., 2021), emergent plants from Lake Wuliangsu exhibited a predominance of *n*-C_{27} and *n*-C_{29} alkanes, low concentrations of even-numbered chain *n*-alkanes, and under-detectable *n*-C_{31} alkane, resulting in lower P_{aq} (0.43) and higher CPI (10.24) values. The *n*-alkanes of emergent plants were more depleted in ^{13}C (–34.0‰ to –36.6‰). The up to ~10‰ difference of $\delta^{13}C$ values of *n*-alkanes between submerged macrophytes and emergent plants might be attributed to their different photosynthesis pathways, considering that submerged macrophytes use HCO_3^- as carbon source for photosynthesis, whereas emergent plants use CO_2 as the primary carbon source (Chappuis et al., 2017). The riverine sediments were characterized by a higher abundance of long-chain *n*-alkane homologues (i.e., *n*-C_{29} and *n*-C_{31}), resulting in a much lower P_{aq} value (0.20). Moreover, the relative concentrations of even-numbered *n*-alkanes in riverine sourced sediments were relatively higher than those from both aquatic plants, resulting in a slightly lower CPI value (6.03). The $\delta^{13}C$ values of *n*-alkanes from the riverine sediment range from –30.7‰ to –33.1‰, suggesting that the riverine sourced OC might be mainly derived from C_3 plants (Meyers, 2006).

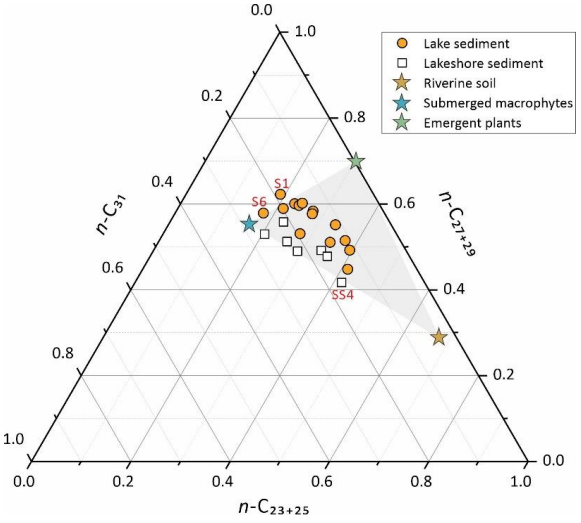

Figure 4. Ternary diagrams of relative percentage of *n*-C_{23}+*n*-C_{25}, *n*-C_{27}+*n*-C_{29}, and *n*-C_{31} relative to *n*-$C_{23+25+27+29+31}$ for all samples including lake surface sediments (orange dots), lakeshore sediments (white squares), riverine soil and aquatic plants (stars).

The notion of quantitative/semi-quantitative methods based on distribution patterns and $\delta^{13}C$ values of *n*-alkane was further supported by the results of lake sediment samples. Firstly, on the ternary diagram of the relative abundance of *n*-C_{23+25}, *n*-C_{27+29}, *n*-C_{31} to *n*-$C_{23+25+27+29+31}$ alkanes (%C_{23+25}, %C_{27+29}, and %C_{31}), most lake sediments roughly fall into the area delineated by the three end-members of submerged macrophytes, emergent plants, and riverine soil (Figure. 4). Secondly, all the $\delta^{13}C$ values of mid- and long-chain *n*-alkanes from surface sediments also roughly fall into the $\delta^{13}C$ range among these

https://doi.org/10.5194/bg-2023-134
Preprint. Discussion started: 17 August 2023

three end-members (–24.0‰ to –36.7‰, supplementary Table S1). Thirdly, more positive $\delta^{13}C$ values were observed in *n*-C_{23} and *n*-C_{25} homologues than *n*-C_{29} and *n*-C_{31} homologues for all sediment samples, tentatively suggesting a major contribution of mid-chain *n*-alkanes from submerged macrophytes as well as contributions from emergent plants and terrestrial plants in long-chain *n*-alkanes (Table S1). These pieces of evidence together demonstrate mixture sources of surface sedimentary OC from submerged macrophytes, emergent plants, and riverine materials, which were also widely recognized by previous studies from bulk characteristics of OC (i.e., Sun et al., 2006; Tian et al., 2011; Fu et al., 2013; Geng et al., 2021). Therefore, the distribution pattern and the $\delta^{13}C$ values of mid- and long-chain *n*-alkanes showed great potential to semi-quantitatively/quantitatively differentiate contribution among various sedimentary OC sources in Lake Wuliangsu.

4.2 Quantification on allochthonous and autochthonous OC by end-member mixing models

4.2.1 Model #1: solely based on distribution patterns of n-alkanes

Firstly, we developed a three end-member model solely based on distribution pattern (i.e., %*n*-C_{23+25}, %*n*-C_{27+29}, and %*n*-C_{31}, Figure 5), to quantitatively estimate the relative contributions of allochthonous and autochthonous OC sources to the sediments within Lake Wuliangsu. Basically, the relative contributions of OC from submerged macrophytes, emergent plants, and riverine sources (F_{sub}, F_{emer}, and F_{riv}) can be calculated by Eq. (3)–(6) listed in Supplementary Material. Sample S1, S6, and SS6 fall slightly outside the area circled by the three sources, we assigned F_{sub} values of samples S1 and S6 to 0, whereas F_{emer} value of sample SS6 to 0.

The results of Model #1 show that the relative contributions of mid- and long-chain *n*-alkanes from submerged macrophytes, emergent plants, and riverine sources to lake surface sediments were 15.2% (0%–42.9%), 31.8% (14.3%–42.6%), and 53.0% (34.5%–68.6%), respectively. The relative contributions of mid- and long-chain *n*-alkanes from submerged macrophyte, emergent plant, and riverine soil to lakeshore sediments were 20.1% (8.4%–32.7%), 9.4% (0%–18.6%), and 70.5% (53.1%–91.0%), respectively. The major contributions of riverine sourced OC to the *n*-alkane pool in both lake sediments and lake shore sediments seem to contradict with the conclusion that sedimentary OC is mainly of autochthonous origins within Lake Wuliangsu (Sun et al., 2006; Tian et al., 2011; Fu et al., 2013).

As the CPI values and $\delta^{13}C$ values of *n*-alkanes are independent with the distribution pattern of *n*-C_{23} to *n*-C_{31} alkanes, they could be applied to test whether this model was valid or not. We calculated the estimated CPI (CPI_{est}) values and $\delta^{13}C$ values of every single *n*-alkane component ($\delta^{13}C_{i\text{-}est}$) based on the results of this mixing Model #1, by Eq. (7) and (8) listed in Supplementary Material. On one hand, the CPI_{est} values for the lake sediments and lakeshore sediments were linearly correlated with the CPI values (r^2=0.45, n=20, $p < 0.01$, Figure. 5a), but with slightly different from the absolute values (difference of –4.60 to 9.85). Specially, the samples with lower CPI_{est} values than the actual CPI values are mainly from open-water areas (e.g., sites S3, S11, S12, S13, and S14), tentatively indicating that this mixing model might underestimate the contribution of submerged macrophyte OC at these sites.

https://doi.org/10.5194/bg-2023-134
Preprint. Discussion started: 17 August 2023

Although the CPI_{est} values for lake sediments also show positive correlation with actual CPI values (r^2=0.59, n=14, p<0.01), those for lakeshore sediments show very weak but negative correlation with actual CPI values (r^2=0.16, n=6). Therefore, the end-member mixing model solely based on distribution patterns of *n*-alkanes might not be applicable for the lakeshore areas, considering that the relative concentration of odd and even-chain *n*-alkanes have altered caused by complex microbial degradation behavior and OC sources. On the other hand, the estimated $\delta^{13}C$ values of every single *n*-alkane exhibited a significant correlation with the actual $\delta^{13}C$ values (r^2= 0.36, n=100, p < 0.01, Figure. 5b), but also showed slightly different absolute values (difference of -4.1‰ to 6.0‰). The data biasing the 1:1 line for the estimated and the actual $\delta^{13}C$ values with 2‰ uncertainty is mainly from $\delta^{13}C$ values of submerged macrophyte-sourced *n*-alkanes (i.e., *n*-C_{25}) from sites S1, S3–S5, S7, S9 and S11–S14, and $\delta^{13}C$ values of *n*-C_{27}, *n*-C_{29} and *n*-C_{31} alkanes from lake sediments mainly at the open-water areas (sites S3, S11, S12, S13 and S14, Figure. 5b). Accordingly, results from Model #1 seem to underestimate the relative contributions from submerged macrophytes, consistent with what was found from the comparison of CPI_{est} and actual CPI values.

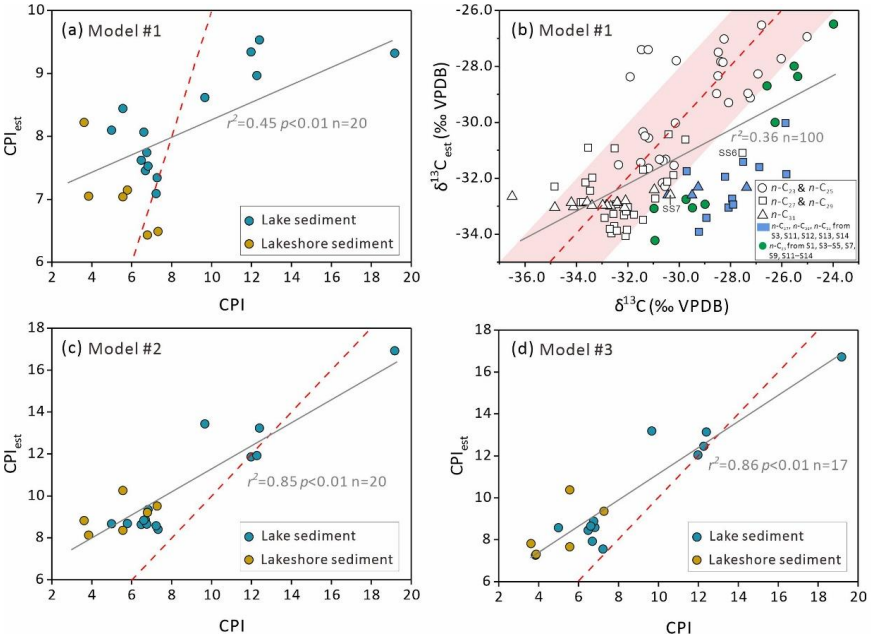

Figure 5. Plots of (a) actual CPI values *vs.* CPI_{est} values calculated by Model #1, (b) actual $\delta^{13}C$ values *vs.* estimated $\delta^{13}C$ values of *n*-C_{23} to *n*-C_{31} calculated by Model #1 (blue colored refer to *n*-C_{27}, *n*-C_{29} and *n*-C_{31} from open water area, e.g. S3, S11, S12, S13, and S14, and green colored refer to *n*-C_{25} from S1, S3-S7, S9, and S11-S14), (c) actual CPI values *vs.* CPI_{est} values calculated by Model #2, and (d) actual CPI values *vs.* CPI_{est} values calculated by Model #3, respectively from sediments profile of Lake Wuliangsu. The red dashed line represents 1:1 correlation between CPI_{est} values and actual CPI vales. The linear regression line is shown in gray.

In summary, Model #1 solely based on the distribution pattern of *n*-alkanes can only track the spatial variation of the

https://doi.org/10.5194/bg-2023-134
Preprint. Discussion started: 17 August 2023

relative contributions of submerged macrophytes, emergent plants, and riverine sources within the lake rather than the surrounding catchment. Even though, there might be large uncertainty in the absolute value from this model. The potential reason might be the insufficient samples for the end-member determination and more samples from aquatic species and riverine sources are needed. Another reason is that the microbially mediated degradation on shorter chain *n*-alkanes during the transportation and depositional processes, which to some extent resulting in relatively higher contribution from *n*-alkanes of longer chains (i.e., signature from emergent plants and riverine sourced OC, Van Beilen et al., 2003; Wang et al., 2019). Both difficulties might be constrained by the introduction of the $\delta^{13}C$ values of *n*-alkanes.

4.2.2 Model #2: introducing the $\delta^{13}C$ values of n-alkanes into the mixing model

We further developed another end-member mixing model for lake surface sediments (Model #2) together with the $\delta^{13}C$ values of *n*-C_{23} to *n*-C_{31} alkanes. For the F_{sub}, we first listed all the possible cases with f_{emer}/f_{riv} ranging from 0 to infinity, and calculated the averaged F_{sub} value for all possible F_{sub} values following Eq. (9)–(11) listed in Supplementary Material. Similarly, for the F_{emer}, we first listed all the possible cases with f_{sub}/f_{riv} ranging from 0 to infinity, and calculated the averaged F_{emer} value for all possible F_{sub} values f_{emer} following Eq. (12)–(14) listed in Supplementary Material, and then F_{riv} was calculated by Eq. (15).

According to Model #2, relative contributions of mid- and long-chain *n*-alkanes from submerged macrophytes, emergent plants, and riverine sources in lake surface sediments were 42.1% (14.0%–95.5%), 26.1% (1.9%–43.4%), and 31.8% (2.6%–44.5%), respectively (Supplementary Table S3). The relative contributions of mid- and long-chain *n*-alkanes from submerged macrophytes, emergent plants, and riverine sources to lakeshore sediments were 29.3% (12.9%–48.5%), 30.8% (13.8%–50.6%), and 40.0% (30.9%–47.9%), respectively (Supplementary Table S3). Compared to the results from Model #1, the ones from Model #2 showed lower riverine OC contribution (avg. 34.3% *vs.* 58.3%), slightly higher emergent plant contribution (avg. 27.5% *vs.* 25.1%), and much higher submerged macrophyte contribution (avg. 38.2% *vs.* 16.7%). Besides that, the spatial variation patterns of the relative contributions from different OC sources are quite similar, as illustrated by strong correlations of the same proxy between both models (r^2=0.61 and 0.50 for F_{sub} and F_{riv}, n=20, p<0.01). Specifically, the contribution of submerged macrophytes was relatively higher at sites S3, S11, S12, S13, S14, and SS7 in Model #2, in agreement with the results from Model #1. Therefore, both independent models might be capable to track the spatial characteristics of allochthonous and autochthonous OC contributions to the Lake Wuliangsu sediments but show different absolute values for both submerged macrophytes and riverine soils.

We also calculated the CPI_{est} values based on the results of Model #2 to test whether this model was valid or not (Supplementary Table S3). The CPI_{est} values more significantly correlated with the actual CPI values in Model #2 than Model #1 (r^2=0.85, n=20, p<0.01, Figure. 5c). The CPI_{est} values from lakeshore sediments in Model #2 also show weak positive correlation with actual CPI values (r^2=0.26, n=6), much more reasonable than those from Model #1 (Figure. 5a). The absolute

https://doi.org/10.5194/bg-2023-134
Preprint. Discussion started: 17 August 2023

CPI_{est} values from Model #2 are much closer to the real CPI values than those from Model #1 (differences of –4.71 to 2.26 vs. –4.60 to 9.85), suggesting that Model #2 might be more convincing in terms of the absolute values. Indeed, between the two models, higher contributions from submerged macrophytes occurred in samples located in the open-water area (sites S3, S11, S12, S13, and S14) inferred by Model #2 (62.2%–95.5%) should be more rational. Especially for sample S3, results from Model #2 demonstrated that sedimentary *n*-alkanes were almost exclusively contributed by submerged macrophytes (95.5%), potentially explaining why this sample deviating the linear correlation between the total concentration of *n*-alkanes and TOC value by its much higher *n*-alkanes concentrations (Figure. 2b). In this sense, introducing the $\delta^{13}C$ signatures into the models of *n*-alkanes to reduce the potentially large error brought from uncertainties of the distribution patterns in the sourced appointment.

4.2.3 Model #3: combination of both Model #2 and Model #3

In Model #2, we initially listed all possibilities of f_{emer}/f_{riv} ranging from 0 to infinity, and calculated the average value of F_{sub}, F_{emer}, and F_{riv}. In this way, uncertainties would be produced, as possibilities of different f_{emer}/f_{riv} are not weighted by other methods. In this sense, we attempted to fixed f_{emer}/f_{riv} to the F_{emer}/F_{riv} values that calculated from Model #1, and calculate F_{sub} based on Eq. (9)–(11), and then calculate F_{emer} and F_{riv} based on Eq. (16)–(17) listed in Supplementary Material. In this model we excluded samples S1, S6, and SS6 from the end-member mixing model to avoid potentially improper estimation, considering their results derived from Model #1 are partially unreliable.

The results from this updated Model #3 show that the relative contributions of mid- and long-chain *n*-alkanes from submerged macrophytes, emergent plants, and riverine sources in lake surface sediments were 43.9% (13.0%–95.3%), 22.4% (1.2%–37.2%), and 33.7% (3.6%–61.3%), respectively (Supplementary Table S3). The relative contributions of mid- and long-chain *n*-alkanes from submerged macrophytes, emergent plants, and riverine sources to lakeshore sediments were 34.5% (20.8%–56.4%), 9.8% (2.0%–16.9%), and 55.6% (34.4%–73.5%), respectively (Supplementary Table S3). Results from this updated Model #3 are strongly correlated with those from Model #2 results (r^2=0.95 and 0.81 for submerged macrophytes and riverine OC, n=17, $p < 0.01$). Also, the CPI_{est} values from Model #3 showed significantly correlated with those from Model #2 (r^2=0.97, n=17, p<0.01), and are strongly correlated with the actual CPI values (r^2=0.86, n=17, p<0.01, Figure. 5d). The absolute CPI_{est} values from Model #3 are also much closer to the actual CPI values than those from Model #1 (differences of –4.83 to 2.46 vs. –4.60 to 9.85). This means that once $\delta^{13}C$ signatures of *n*-alkanes were introduced (i.e., Model #2 and Model #3), the end-member mixing models would be relatively stable no matter how we calculate the f_{emer}, f_{sub}, and f_{riv} values. Therefore, all three models might be all adequate for the evaluation of spatial variation patterns of different OC sources of Lake Wuliangsu, and Models #2 and Model #3 would be more convincing with respect to discuss the absolute values.

https://doi.org/10.5194/bg-2023-134
Preprint. Discussion started: 17 August 2023

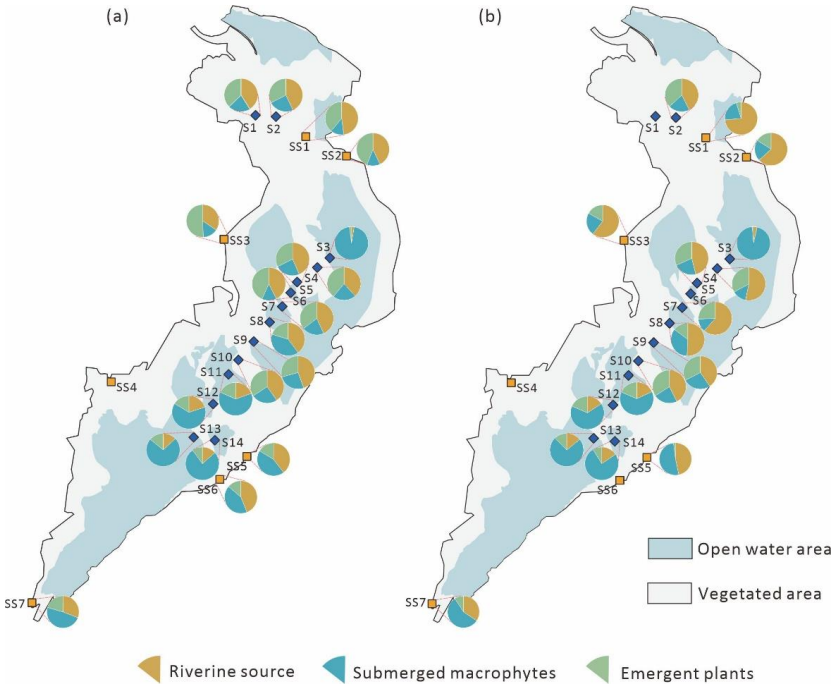

Figure 6. Pie charts of OC contributions from riverine soil (yellow segment), submerged macrophytes (blue segment), and emergent plants (light-green segment) for lake and lakeshore surface sediments from Lake Wuliangsu calculated by (a) Model #2 and (b) Model #3.

400

4.3 Spatial characteristics of allochthonous and autochthonous OC within Lake Wuliangsu

According to the results of both Model #2 and Model #3, the relative contribution of riverine sourced OC to sedimentary *n*-alkanes demonstrated a clear decreasing trend from the lake center (S7 and S8, 11.6%–12.4% from Model #2 and 18.5%–21.0% from Model #3) to the southern part (S13 and S14, 3.6%–4.0% from Model #2 and 4.0%–4.6% from Model #3, Figure. 6). In terms of the absolute contributions to sedimentary OC calculated by Eq. (18)–(20) listed in Supplementary Material, OC derived from riverine input was higher at sites S7 and S8 (0.57%–0.60% from Model #2 and 0.85%–1.09% from Model #3, Figure. 7), and exhibited a decreasing trend to the southward until it reaches the lowest values at site S14 (0.06% from Model #2 and Model #3). Therefore, a large amount of riverine sourced OC from the main channel has settled down during the southward migration process (Fu et al., 2013). This notion was also supported by the gradual transition of the sedimentary grain size from sandy silt near the main inlet channel to fine grain at the off-shore areas of Lake Wuliangsu (Yang et al., 2009). On the one hand, once transported to Lake Wuliangsu, the majority of riverine OC can be quickly deposited in regions close to the main inlet channel by hydrological sorting due to quick diminished of the hydrodynamics (near site S6, Zhang et al., 2010), with minor riverine OC further transporting to the southern outlet of Lake Wuliangsu. On the other hand, emergent plant belt at the vegetated areas would also block the coarse particles from further transportation due to its robust underground

https://doi.org/10.5194/bg-2023-134
Preprint. Discussion started: 17 August 2023

415 rhizome system (Zhao et al., 2012). Interestingly, the riverine sourced OC at samples located at the southern open-water of Lake Wuliangsu (sites S12–S14, riverine sourced OC of 0.06%–0.41%, TOC of 4.45%–7.19%) are very low and are close to those from lake sediments at the northern section (sites S1 and S2, riverine sourced OC of 0.10%–0.20%, TOC of 0.64%–0.88%) and lakeshore sediments surrounding the lake (sites SS1–SS7, riverine sourced OC of 0.02%–0.31%, TOC of 0.15%–1.30%, Figure. 7). Considering that lake sediments at the northern section and lakeshore sediments surrounding the lake are 420 characteristic by relatively stronger hydrodynamics, lower TOC values, and less impact from the riverine input from the channels in the western main inlet channel, most of the riverine sourced OC from the western main inlet channel have been deposited within Lake Wuliangsu, at least before reaching to sites S12–S14. Therefore, lake Wuliangsu may be act as an important trap and sink for allochthonous OC. The soil materials transported to the Middle and the Lower Yellow River Reaches from Lake Wuliangsu might be mainly from the catchment instead of the Upper Yellow River Reaches.

425 For the autochthonous OC, they contribute higher to sedimentary *n*-alkanes than riverine sourced OC for all samples (avg. 65.7% from Model #2 and 59.9% from Model #3). For sites located in the open-water area (sites S3, S11, S12, S13, and S14), autochthonous OC show predominated contributions to sedimentary *n*-alkanes (80.0%–97.4% from Model #2 and 81.9%–96.5% from Model #3), with a major contribution from submerged macrophytes (62.2%–95.5% from Model #2 and 63.4%–95.3% from Model #3) and minor from emergent plants (1.5%–18.2% from Model #2 and 1.2%–18.5% from Model #3). For 430 the rest of the lake surface sediments, autochthonous OC are still the main contributors for sedimentary *n*-alkanes of Lake Wuliangsu (55.5%–61.5% from Model #2 and 47.1%–59.5% from Model #3), with roughly comparable contribution from both submerged macrophytes (14.0%–39.8% from Model #2 and 13.7%–34.6% from Model #3) and emergent plants (20.3%–43.4% from Model #2 and 14.7%–37.2% from Model #3). In lakeshore sediments, contributions from autochthonous OC to sedimentary *n*-alkanes are similar to the lake surface sediments outside the open-water area (52.1%–69.1% from Model #2 435 and 26.5%–65.6% from Model #3).

In terms of the absolute contributions to sedimentary OC (Figure. 7), the contribution of both submerged macrophyte-derived OC and emergent plant-derived OC are strongly coupled with the bulk TOC values (e.g., r^2=0.71 and 0.62, n=20 from Model #2, and r^2=0.72 and 0.66, n=17 from Model #3, p<0.01), further supplementary the notion that the sedimentary OC of Lake Wuliangsu is mainly of the autochthonous source. Specifically, submerged macrophytes contribute much higher in the 440 open-water areas from northern part (site S3, 3.71% from Model #2 and 3.76% from Model #3) and southern part (sites S11, S12, and S13, 3.04%–4.39% from Model #2 and 3.13%–4.30% from Model #3). The contribution of submerged macrophytes-derived OC showed an increasing trend from the central section (site S4) to the southern part (sites S11–S13, Figure. 7), consistent with the spatial distribution pattern of submerged macrophytes as inferred by the P_{aq} values (Figure. 2) from the same samples and the results from the on-site investigations (Du et al., 2022). For sites along the central to southern section 445 (sites S6–S13), contributions of the emergent plant-derived OC are higher (1.16–3.61% from Model #2 and 1.14–3.33% from Model #3). Therefore, higher contributions of submerged macrophytes are usually observed in the open-water area, while

https://doi.org/10.5194/bg-2023-134
Preprint. Discussion started: 17 August 2023

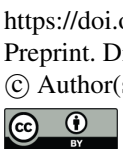

higher contributions of emergent plants in the central part and southern part of lake across both the vegetated area and the open-water area. Such results are consistent with the remote sensing data and on-site investigations (Yu et al., 2007; Bao et al., 2016), which suggest that major contributions of emergent plants to OC deposition and stronger difference among areas with different water depth and distances to the lake shore.

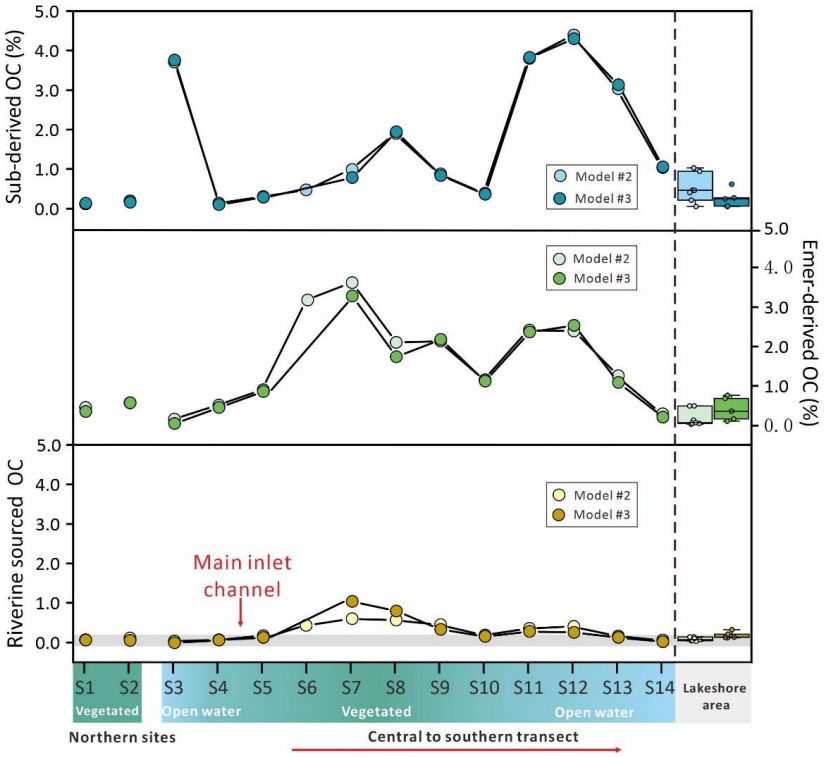

Figure 7. Absolute OC contributions from submerged macrophytes, emergent plants, and riverine soil calculated by Model #2 and Model #3. For lake shore samples, data were shown in box plot. The boxes, the horizontal lines within boxes, and the whiskers indicate the interquartile range, median values, and minimum and maximum values, respectively.

Theoretically, water transparency, water depth, and nutrient concentrations are the key parameters affecting the growth of submerged macrophytes and emergent plants. With stable hydrological conditions and less anthropogenic disturbances in the open-water areas (sites S3, S11, S12, and S13, Tian et al., 2020), higher light energy transmission in clear water body could favor the growth of submerged macrophytes (Heidbuechel et al. 2019). In the case of Lake Wuliangsu, submerged macrophytes grow quickly in the ice-free seasons, and experience massive death, corruption, and deposition during the frozen season, eventually promoting strong OC burial (Huang et al., 2015). By contrast, low biomass of submerged macrophytes was observed at regions close to main channel with low water transparency, largely due to the stronger sediment resuspension under intensive hydrodynamics (Du et al., 2022). Interestingly, the open-water areas located at the central part (sites S11, S12, and S13) show

https://doi.org/10.5194/bg-2023-134
Preprint. Discussion started: 17 August 2023

both relatively higher water transparency and water depth (Tian et al., 2020), we suspect that the water depth and offshore distance also act an important role for water transparency. As emergent plants contribute similarly in the central and southern sections of lake across both the vegetation-covered area and the open-water area, the water transparency and water depth might not be the major factors for the growth of the emergent plants (Yu et al., 2007). Considering Lake Wuliangsu is generally shallow (1–1.5 m) under current intense paludification, the whole lake might be all suitable for the emergent plants to grow.

Interestingly, at northern sites with relatively higher contribution of emergent plants over submerged macrophytes (sites S1 and S2), the absolute TOC are lower, tentatively suggesting that the productions of emergent plants might be controlled by factors from the central and the south. Therefore, we believe that higher concentrations of NH_4^+ and PO_4^{3+} from the agricultural farmland could trigger the bloom of submerged macrophytes and emergent plants (Ciurli et al., 2009), as inferred by higher OC contributions from both submerged macrophytes and emergent plants at sites S11, S12, and S13 corresponding to higher nitrogen and phosphorous concentrations. The decomposition of litters could continuously release the nutrients (Wu et al., 2011), creating a positive feedback loop for the submerged macrophytes to nourish. However, much higher concentrations of NH_4^+ and PO_4^{3+} at this region might somehow hinder the submerged macrophytes and emergent plants from prospering (Liu et al., 2020). Therefore, to improve the ecological conditions and OC burial of Lake Wuliangsu, it is necessary to supervise and manage the quality of the inflowing water from the agricultural farmland, as well as preservation of the water body from current intense paludification.

4.4 Effect of OC sources to heterotrophic microbial activities in Lake Wuliangsu

Among all OC mineralization processes, heterotrophic microbial attack on OC has been considered to be one of the most critical factors in determining the sinking efficiency of OC in lakes (Mayer et al., 2006; Sun et al., 2022). Therefore, investigations on heterotrophic microbial activities response to different types of OC sources would have important implications in environmental management with respect to OC source-sink behaviors. A previous study suggested that branched glycerol dialkyl glycerol tetraethers (brGDGTs) and GDGT-0 in Lake Wuliangsu should be mainly produced by heterotrophic anaerobic bacteria (*Acidobacteria*) and methanogenic archaea (*Euryarchaeota*) within the lake, while crenarchaeol from the soil OC transported through the Yellow River system (He et al., 2023). Accordingly, the BIT values of lake surface sediments in Lake Wuliangsu are very close to 1.0 (He et al., 2023), while the BIT values in soil and riverine samples collected in the Yellow River Reaches (0.81, Wu et al., 2014; Yang et al., 2014). $BR_{in\text{-}situ/soil}$ ratio calculated from the BIT values can be used to quantitatively evaluate the activities of *in-situ* heterotrophic anaerobic bacteria (*Acidobacteria*) to overall microorganisms (He et al., 2023). Also, a diagnostic method by GDGT-0/crenarchaeol values ($R_{0/5}$) can be used for identification of the methanogenic *Euryarchaeota* ($R_{0/5}$ >2, Blaga et al., 2009; He et al., 2023).

When comparing our quantitative evaluation of the submerged macrophytes, emergent plants, and riverine sourced OC values with the $R_{0/5}$ and $BR_{in\text{-}situ/soil}$ ratio, we observe a strong correlation between the submerged macrophyte-sourced OC and

https://doi.org/10.5194/bg-2023-134
Preprint. Discussion started: 17 August 2023

both the $R_{0/5}$ and $BR_{in\text{-}situ/soil}$ ratios (r^2=0.68 and r^2=0.81, p<0.01, n=33, Figure. 8a–b, Supplementary Table S4), and no correlation between emergent plant-sourced OC *vs*. both the $R_{0/5}$ and $BR_{in\text{-}situ/soil}$ ratios (r^2=0.04 and r^2=0.10, n=33, Figure. 8c–d), and riverine sourced OC vs. both the $R_{0/5}$ and $BR_{in\text{-}situ/soil}$ ratios (r^2=0.02 and r^2=0.07, n=33, Figure. 8c–d). In addition, samples in the open-water zone usually show much higher $R_{0/5}$ and $BR_{in\text{-}situ/soil}$ ratios than vegetated zones (79.17 *vs*. 26.13 and 84.82 *vs*. 26.24 for $R_{0/5}$ and $BR_{in\text{-}situ/soil}$, respectively). These evidences suggest that the open water zones create ideal conditions for heterotrophic anaerobic bacteria and methanogenic *Euryarchaeota* than the vegetated covered areas. Reasons for the phenomenon should be related to the geochemical and ecological properties of submerged macrophytes, and the environmental characteristics of open water zone. Firstly, compared with emergent plants and terrestrial plants, organic compounds sourced from submerged macrophytes are more labile and easier to be degraded in the water column and surface sediments (Bastviken et al., 2003; Chimney and Pietro, 2006), creating a more anaerobic condition in places where the submerged macrophytes habitat (i.e. open water zone). Secondly, dense stands of submerged macrophytes could also provide more suitable substrates for methanogenic archaea to produce CH_4 (Hilt et al., 2022), as evidenced by higher CH_4 fluxes in the open water zones than vegetated areas of Lake Wuliangsu (Li et al., 2022). Such a notion is also supported by the incubation experiments showing that submerged macrophytes had higher CH_4 production than terrestrial debris in an anoxic sedimentary system (Grasset et al., 2018). Thirdly, considering that the open-water zone usually occurs in the offshore region with relatively higher water depth (Li et al., 2022), we believe that the higher water depth and distance to the lake shore would both potentially promote the development of anoxia conditions for methanogenic *Euryarchaeota* and anaerobic bacteria. Fourthly, when Lake Wuliangsu was skimmed with ice in the winter season, massive dead submerged macrophyte debris was deposited in the lake bottom, further consuming the dissolved oxygen availability in water column, which can be hardly recharged due to the frozen situation on the lake surface (Sun et al., 2022; Zhang et al., 2022). All these reasons together lead to higher activities of heterotrophic anaerobic bacteria and methanogenic *Euryarchaeota* in the open water zone observed in our data.

Interestingly, when the samples located at the open-water zone with predominated submerged macrophyte contributions are excluded (sites S3, S11, S12, S13, and S14), strong correlations can be also observed for the contributions of the riverine sourced OC *vs*. both the $R_{0/5}$ and $BR_{in\text{-}situ/soil}$ ratios (r^2=0.78 and r^2=0.82, respectively, p<0.01, n=25) and the emergent plant-sourced OC vs. both the $R_{0/5}$ and $BR_{in\text{-}situ/soil}$ ratios (r^2=0.81 and r^2=0.74, respectively, p<0.01, n=25) (Figure. 8c–d). Indeed, results from a sedimentary core drilled in Lake Wuliangsu also show strong positive correlations for both the TOC values and the $R_{0/5}$ values during AD 1831–1972 and the TOC values and the $BR_{in\text{-}situ/soil}$ values AD 1831–2007 (He et al., 2023). In this sense, regardless of OC types, higher OC input are prone to consume the dissolved oxygen in the water body, and eventually create anaerobic conditions in freshwater systems for heterotrophic anaerobic microorganisms to prosper (Grasset et al., 2018). However, as mentioned above, the submerged macrophytes conduct a much stronger effect on the heterotrophic anaerobic microbial activities. Therefore, the amount and more significantly the sources of OC can shape the microbial communities and reactivities, which would also play important roles in organic carbon cycle in shallow lake systems.

https://doi.org/10.5194/bg-2023-134
Preprint. Discussion started: 17 August 2023

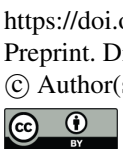

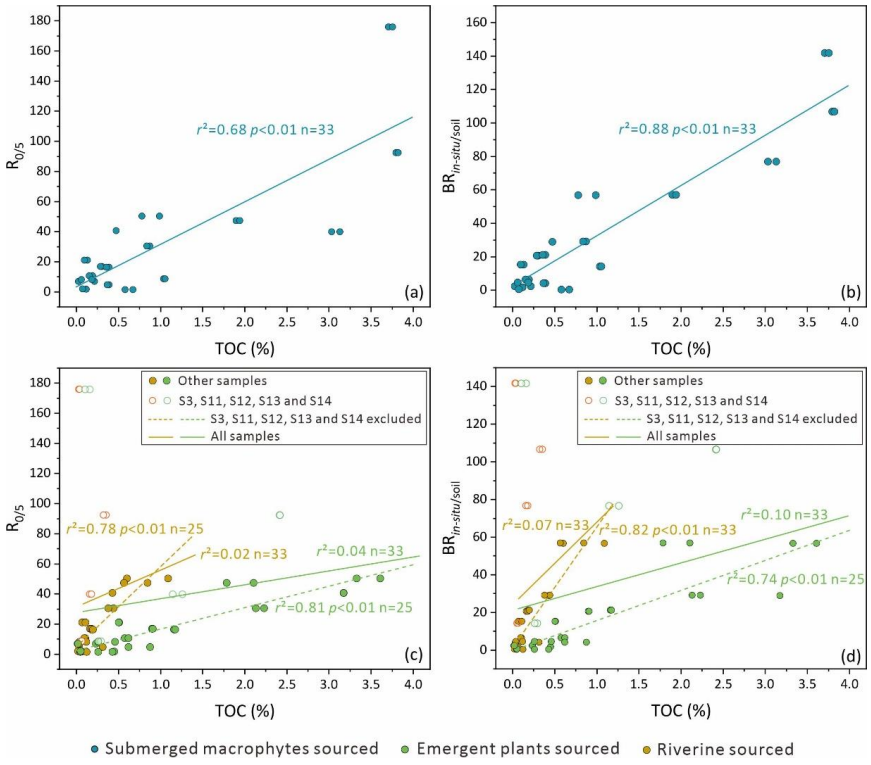

Figure 8. Plots of (a) OC values derived from submerged macrophytes *vs.* $R_{0/5}$ values, (b) OC values derived from submerged macrophytes *vs.* $BR_{in\text{-}situ/soil}$ values, (c) OC values derived from emergent plants and riverine soil *vs.* $R_{0/5}$ values (d) OC values derived from OC values derived from emergent plants and riverine soil *vs.* $BR_{in\text{-}situ/soil}$ values . The linear regression line including all samples shown in solid line. The linear regression line excluding S3, S11, S12, S13, and S14 shown in dashed line.

5. Conclusions

Our analyze of the distribution pattern and $\delta^{13}C$ value of *n*-alkanes from lake surface sediments yielded new insights about the OC appointment of Lake Wuliangsu with anthropogenic-induced paludification conditions. The findings highlight the potential importance of quantifying contribution from different sources to the sedimentary OC pool.

1) Submerged macrophytes, emergent plants, and riverine soil show their unique distribution patterns and $\delta^{13}C$ signatures of *n*-alkanes. In this sense, end-member mixing models were developed to quantify OC sources within lake. Compared to the model based on distribution patterns of *n*-alkanes, the $\delta^{13}C$ values could effectively reduce the potential uncertainty of the model.

2) The model results suggest that the amount of riverine sourced OC from the main channel to Lake Wuliangsu have been settled down during the southward migration process. Therefore, Lake Wuliangsu serves as an important trap and sink for allochthonous OC from the Upper Yellow River Reaches. The model results also show a predominant contribution from the

https://doi.org/10.5194/bg-2023-134
Preprint. Discussion started: 17 August 2023

545 autochthonous OC to Lake Wuliangsu, with the open-water area dominated by submerged macrophytes and the rest of the areas by emergent plants. The spatial distribution pattern of autochthonous OC might be mainly controlled by water transparency, water depth, and nutrient concentrations.

3) Open-water areas dominated by submerged macrophytes might be more favorable for heterotrophic anaerobic bacteria and methanogenic archaea, largely due to active recycling processes for the labile OC derived from submerged macrophytes.

550

Author Contributions

Y.H. and design research and is responsible for the project. Y.H. and A.Z. collected the samples. Q.Z. and Y.H. performed laboratory analyses. Q.Z. and Y.H. analyzed the data. Q.Z. and Y.H. wrote the initial draft of the manuscript. All authors edited subsequent versions of the manuscript and approved the final submission.

555

Acknowledgments

We thank Prof. Yongge Sun for constructive suggestions on writing this paper. This study was supported by National Natural Science Foundation of China (41877332, 42073071).

Competing Interests

560 The authors declare that they have no conflict of interest.

Data availability

The data that support the findings of this study are presented in the supplementary Table.

https://doi.org/10.5194/bg-2023-134
Preprint. Discussion started: 17 August 2023

References

1. Ahad J. M. E., Ganesharm, R. S., Bryant, C. L., Cisneros, L. M., Ascough, P., Fallick, A. E., and Slater, G. F.: Sources of *n*-alkanes in an urbanized estuary: insights from molecular distributions and compound-specific stable and radiocarbon isotopes, Mar. Chem., 126, 239–249. https://doi.org/10.1016/j.marchem.2011.06.002, 2011.
2. Aichner, B., Herzschuh, U., and Wilkes, H.: Influence of aquatic macrophytes on the stable carbon isotopic signatures of sedimentary organic matter in lakes on the Tibetan Plateau, Org. Geochem., 41, 706–718, https://doi.org/10.1016/j.orggeochem.2010.02.002, 2010.
3. Alahuhta, J., Kanninen, A. K., Hellsten, S., Vuori, K. M., Kuoppala, M., and Hämäläinen, H.: Variable response of functional macrophyte groups to lake characteristics, land use, and space: implications for bioassessment, Hydrobiologia, 737, 201–214, https://doi.org/10.1007/s10750-013-1722-3, 2014.
4. Andrae, J. W., Mclnerney, F. A., and Sniderman, J. M. K.: Carbon isotope systematics of leaf wax *n*-alkanes in a temperate lacustrine depositional environment, Org. Geochem., 150, 104121, https://doi.org/10.1016/j.orggeochem.2020.104121, 2020.
5. Bao, H., Zhuo, Y., Liu, H., Liu, D., Qing, H., Wen, L., and Wang, L.: Estimation of RS-based Biomass of Phragmites communis in Wetland of the Ulansuhai Lake, Arid Zone Res., 33, 1028–1035, https://doi.org/10.13866/j.azr.2016.05.16, 2016.
6. Bastviken, D., Olsson, M., and Tranvik, L.: Simultaneous measurements of organic carbon mineralization and bacterial production in oxic and anoxic lake sediments, Microb. Ecol., 46, 73–82, https://doi.org/10.1007/s00248-002-1061-9, 2003.
7. Botrel, M., and Maranger, R.: Global historical trends and drivers of submerged aquatic, Glob. Change Biol., 29, 2493–2509, https://doi.org/10.1111/gcb.16619, 2023.
8. Blaga, C. I., Reichart, G. J., Heiri, O., and Sinninghe Damsté, J. S.: Tetraether membrane lipid distributions in water-column particulate matter and sediments: a study of 47 European lakes along a north–south transect, J. Paleolimnol., 41, 523–540, https://doi.org/10.1007/s10933-008-9242-2, 2009.
9. Castañeda, I. S., and Schouten, S.: A review of molecular organic proxies for examining modern and ancient lacustrine environments, Quat. Sci. Rev., 30, 2851–2891, https://doi.org/ 10.1016/j.quascirev.2011.07.009, 2011.
10. Chappuis, E., Seriñá, V., Martí, E., Ballesteros, E., and Gacia, E.: Decrypting stable isotope ($\delta^{13}C$ and $\delta^{15}N$) variability in aquatic plants, Freshw. Biol., 62, 1807–1818, https://doi.org/10.1111/fwb.12996, 2017.
11. Chikaraishi, Y., and Naraoka, H.: $\delta^{13}C$ and δD relationships among three n-alkyl compound classes (*n*-alkanoic acid, *n*-alkane and *n*-alkanol) of terrestrial higher plants, Org. Geochem., 38, 198–215, https://doi.org/10.1016/j.orggeochem.2006.10.003, 2007.
12. Chimney, M. J., and Pietro, K. C.: Decomposition of macrophyte litter in a subtropical constructed wetland in south

https://doi.org/10.5194/bg-2023-134
Preprint. Discussion started: 17 August 2023

595 Florida (USA), Ecol. Eng., 27, 301–321, https://doi.org/10.1016/j.ecoleng.2006.05.016, 2006.

13. Ciurli, A., Zuccarini, P., and Alpi, A.: Growth and nutrient absorption of two submerged aquatic macrophytes in mesocosms, for reinsertion in a eutrophicated shallow lake, Wetland Ecol. Manage., 12, 107–115, https://doi.org/10.1007/s11273-008-9091-9, 2009.

14. Collister James W., Rieley, G., Stern, B., Eglinton, G., and Fry, B.: Compound-specific $\delta^{13}C$ analyses of leaf lipids from
600 plants with differing carbon dioxide metabolisms, Org. Geochem., 21, 619–627, https://doi.org/10.1016/0146-6380(94)90008-6, 1994.

15. Dion-Kirschner, H., McFarlin, J. M., Masterson, A. L., Axford, Y., and Osburn, M. R.: Modern constraints on the sources and climate signals recorded by sedimentary plant waxes in west Greenland, Geochim. Cosmochim. Acta., 286, 336–354, https://doi.org/10.1016/j.gca.2020.07.027, 2020.

605 16. Downing, J. A., Prairie, Y. T., Cole, J. J., Duarte, C. M., Tranvik, L. J., Striegl, R. G., McDowell, W. H., Kortelainen, P., Caraco, N. F., Melack, J. M., and Middelburg, J. J.: The global abundance and size distribution of lakes, ponds, and impoundments, Limnol. Oceanogr., 51, 2388–2397, https://doi.org/10.4319/lo.2006.51.5.2388, 2006.

17. Du, Y., Qing, S., Bao, Y., and Hao, Y.: Spectral features of submerged aquatic vegetation under coverage impact in the Ulansuhai lake, Oceanol. Limnolo. Sin., 53, 74–83, https://doi.org/10.18307/2020.0418, 2022.

610 18. Duan X., Wang, X., Mu, Y., and Ouyang, Z.: Seasonal and diurnal variations in methane emissions from Wuliangsu Lake in arid regions of China, Atmos. Environ., 39, 4479–4487, https://doi.org/10.1016/j.atmosenv.2005.03.045, 2005.

19. Duan, Y., and He, J.: Distribution and isotopic composition of *n*-alkanes from grass, reed and tree leaves along a latitudinal gradient in China, Geochem. J., 45, 199–207, https://doi.org/10.2343/geochemj.1.0115, 2011.

20. Eglinton, G., and Hamilton, R. J.: Leaf epicuticular waxes, Science, 156, 1322–1335,
615 https://doi.org/10.1126/science.156.3780.132, 1967.

21. Ficken, K. J., Li, B., Swain, D. L., and Eglinton. G.: An *n*-alkane proxy for the sedimentary input of submerged/floating freshwater aquatic macrophytes, Org. Geochem., 31, 745–749, https://doi.org/10.1016/S0146-6380(00)00081-4, 2000.

22. Freeman, K. H., Boreham, C. J., Summons, R. E., and Hayers, J. M.: The effect of aromatization on the isotopic compositions of hydrocarbons during early diagenesis, Org. Geochem., 21, 1037–1049, https://doi.org/10.1016/0146-
620 6380(94)90067-1, 1994.

23. Fu, X., Jia, K. Shi, X., Zhao, S., Cui, F., Fan, C., and Gao, H.: The humus composition and distribution of Lake Wuliangsuhai sediments, J. Lake Sci. 25, 489–496, In Chinese. https://doi.org/10.18307/2013.0405, 2013.

24. Geng, Y., Lv, X., Yu, R., Sun, H., Liu, X., Cao, Z., Li, X., Zhu, P., and Ge, Z.: Isotopic characteristics and sources of organic carbon in suspended particulates and sediments in Lake Wuliangsuhai, J. Lake Sci., 33, 1753–1765,
625 https://doi.org/10.1007/s11356-022-24751-6, 2021.

25. Grasset, C., Mendonça, R., Villamor Saucedo, G., Bastviken, D., Roland, F., and Sobek, S.: Large but variable methane

https://doi.org/10.5194/bg-2023-134
Preprint. Discussion started: 17 August 2023

production in anoxic freshwater sediment upon addition of allochthonous and autochthonous organic matter, Limnol. Oceanogr., 63, 1488–1501, https://doi.org/10.1002/lno.10786, 2018.

26. Harpenslager S. F., Thiemer, K., Levertz, C., Misteli, B., Sebola, K., Schneider, S. C., Hilt, S., and Köhler, J.: Short-term effects of macrophyte removal on emission of CO_2 and CH_4 in shallow lakes, Aquat. Bot., 182, 103555, https://doi.org/10.1016/j.aquabot.2022.103555, 2022.
27. He, Y., Sun, D., Wu, J., and Sun, Y.: Factors controlling the past ~150-year ecological dynamics of Lake Wuliangsu in the upper reaches of the Yellow River, Holocene, 25, 1–8, https://doi.org/10.1177/0959683615585841, 2015.
28. He, Y., Zhao, Q., and Sun, D.: Unique distribution pattern and $\delta^{13}C$ signature of *des*-A- triterpenoids from Lake Wuliangsu: source and paleoenvironmental implications, Org. Geochem., 174, 104509, https://doi.org/10.1016/j.orggeochem.2022.104509, 2022.
29. He, Y., Zhao, Q., and Sun, D.: *In-situ* activities of anaerobic bacteria and methanogenic archaea in shallow lakes over the Anthropocene: A case study of Lake Wuliangsu, Chem. Geol., 619, 121312, https://doi.org/10.1016/j.chemgeo.2023.121312, 2023.
30. Heidbuechel, P., Jahns, P., and Hussner, A.: Chlorophyll fluorometry sheds light on the role of desiccation resistance for vegetative overland dispersal of aquatic plants, Freshw. Biol., 64, 1401–1415, https://doi.org/10.1111/fwb.13313, 2019.
31. Hilt, S., Grossart, H. P., McGinnis, D. F., and Keppler, F.: Potential role of submerged macrophytes for oxic methane production in aquatic ecosystems, Limnol. Oceanogr., 67, S76–S88, https://doi.org/10.1002/lno.12095, 2022.
32. Ho, S., Wang, C., Wang, M., and Li, Z.: Effect of petroleum on carbon and hydrogen isotopic composition of long-chain *n*-alkanes in plants from the Yellow River Delta, China, Environ. Earth Sci., 74, 1603–1610, https://doi.org/10.1007/s12665-015-4161-9, 2015.
33. Holtvoeth, J., Whiteside, J. H., Engels, S., Freitas F. S., Grice, K., Greenwood, P., Johnson, S., Kendall, I., Lengger, S. K., Lücke, A., Mayr, C., Naafs, B. D. A., Rohrssen, M., and Sepúlveda, J.: The paleolimnologist's guide to compound-specific stable isotope analysis–an introduction to principles and applications of CSIA for Quaternary lake sediments, Quat. Sci. Rev, 207, 101–133, https://doi.org/10.1016/j.quascirev.2019.01.001, 2019.
34. Huang, X., Li, L., Lu, Y., Pan, G., Qi, Y., Duan, C., and Mei, Y.: Composition and Storage of Organic Carbon in Soils of in Ulansuhai Wetlands in Inner Mongolia Autonomous Region, Wetland Sci., 13, 252–257, https://doi.org/10.13248/j.cnki.wetlandsci.2015.02.018, 2015.
35. Hyun, S., Shin, K. H., Lee, S. C., Chang, S. W., and Nam, S. I.: Terrestrial *n*-alkanes and their carbon isotope records from the Hanon paleo-maar sediment, Jeju Island, Korea: implications for paleoclimate and paleovegetation over the last 35 kyrs, Quat. Int. 441 (Part A), 89–100, https://doi.org/10.1016/j.quaint.2016.08.047, 2017.
36. Li, L., Yao, S., Xue, B., Cheng, L., and Yan, R.: Methane levels in five shallow lakes in China: Effect of lake paludification, Quat. Int., 503, part A, 128–135, https://doi.org/10.1016/j.quaint.2018.08.004, 2019.

https://doi.org/10.5194/bg-2023-134
Preprint. Discussion started: 17 August 2023

37. Li, G., Zhang, S., Shi, X., Zhan, L., Zhao, S., Sun, B., Liu, Y., Tian, Z., Li, Z., Arvola, L., Uusheimo, S., Tulonen, T., and Huotari, J.: Spatiotemporal variability and diffusive emissions of greenhouse gas in a shallow eutrophic lake in Inner Mongolia, China, Ecol. Indic., 145, 109578, https://doi.org/10.1016/j.ecolind.2022.109578, 2022.

38. Liu, J., An, Z. and Liu, H.: Leaf wax *n*-alkane distributions across plant types in the central Chinese Loess Plateau, Org. Geochem., 125, 260–269, https://doi.org/10.1016/j.orggeochem.2018.09.006, 2018.

39. Liu, C., Wang, W., Wu, Y., Zhou, Z., Lai, Q., and Shao, Z.: Multiple alkane hydroxylase systems in a marine alkane degrader, Alcanivorax dieselolei B-5, Environ. Microbiol., 13, 1168–1178, https://doi.org/10.1111/j.1462-2920.2010.02416.x, 2011.

40. Liu, H., and Liu, W.: *n*-Alkane distributions and concentrations in algae, submerged plants and terrestrial plants from the Qinghai-Tibetan Plateau, Org. Geochem., 99, 10–22, https://doi.org/10.1016/j.orggeochem.2016.06.003, 2016.

41. Liu, W., Yang, H., Wang, H., An, Z., Wang, Z., and Leng, Q.: Carbon isotope composition of long chain leaf wax *n*-alkanes in lake sediments: A dual indicator of paleoenvironment in the Qinghai-Tibet Plateau, Org. Geochem., 83-84, 190–201, https://doi.org/10.1016/j.orggeochem.2015.03.017, 2015.

42. Liu, Y., Li, C., Anderson, B., Zhang, S., Shi, X., and Zhao, S.: A modified QWASI model for fate and transport modeling of mercury between the water-ice-sediment in Lake Ulansuhai, Chemosphere., 176, 117–124, https://doi.org/10.1016/j.chemosphere.2017.02.111, 2017.

43. Liu, Y., He, L., Hilt, S., Wang, R., Zhang, H., and Gang, G.: Shallow lakes at risk: Nutrient enrichment enhances top-down control of macrophytes by invasive herbivorous snails, Freshw. Biol., 66, 436–446, https://doi.org/10.1111/fwb.13649, 2020.

44. Lü, C., He, J., Sun, H., Xue, H., Liang, Y., Bai, S., Sun, Y., Shen, L., and Fan, Q.: Application of allochthonous organic carbon and phosphorus forms in the interpretation of past environmental conditions, Environ. Geol., 55, 1279–1289, https://doi.org/10.1007/s00254-007-1076-0, 2008.

45. Ma, L., Wu, J., and Abuduwaili, J.: Geochemical evidence of the anthropogenic alteration of element composition in lacustrine sediments from Wuliangsu Lake, north China, Quat. Int., 306, 107–113, https://doi.org/10.1016/j.quaint.2013.03.021, 2013.

46. Mayer, L. M., Schick, L. L. Skorko, K., and Boss, E.: Photodissolution of particulate organic matter from sediments, Limnol. Oceanogr., 51, 1064–1071, https://doi.org/10.4319/lo.2006.51.2.1064, 2006.

47. Meyers, P. A.: An overview of sediment organic matter records of human eutrophication in the Laurentian Great Lakes region, Water Air Soil Pollut., 6, 453–463, https://doi.org/10.1007/s11267-006-9059-9, 2006.

48. Ni, M., Liang, X., Hou, L., Li, W., and He. C.: Submerged macrophytes regulate diurnal nitrous oxide emissions from a shallow eutrophic lake: A case study of Lake Wuliangsuhai in the temperate arid region of China, Sci. Total Environ., 811, 152451, https://doi.org/10.1016/j.scitotenv.2021.152451, 2022.

https://doi.org/10.5194/bg-2023-134
Preprint. Discussion started: 17 August 2023

49. Shen, B., Wu, J., and Zhao, Z.: A ~150-year record of human impact in the Lake Wuliangsu (China) watershed: evidence from polycyclic aromatic hydrocarbon and organochlorine pesticide distributions in sediments, J. Limnol., 76, 129–136, https://doi.org/10.4081/jlimnol.2016.1529, 2016.

50. Sinninghe Damsté, J. S., Verschuren, D., Ossebaar, J., Blokker, J., Houten, R. V., van der Meer, M. T. J., Plessen, B., and Schouten, S.: A 25,000-year record of climate-induced changes in lowland vegetation of eastern equatorial Africa revealed by the stable carbon-isotopic composition of fossil plant leaf waxes, Earth Planet. Sci. Lett., 302, 236–246, https://doi.org/10.1016/j.epsl.2010.12.025, 2011

51. Sivakumar, M. V. K., Brunini, O., and Das, H. P.: Impacts of Present and Future Climate Variability on Agriculture and Forestry in the Arid and Semi-Arid Tropics, Clim. Change., 70, 31–72, https://doi.org/10.1007/s10584-005-5938-8, 2005.

52. Song, S., Li, C., Shi, X., Zhao, S., Tian, W., Li, Z., Bai, Y., Cao, X., Wang, Q., Huotari, J., Tulonen, T., Uusheimo, S., Leppäranta, M., Loehr, J., and Arvola, L.: Under-ice metabolism in a shallow lake in a cold and arid climate, Freshw. Biol., 64, 1710–1720, https://doi.org/10.1111/fwb.13363, 2019.

53. Struck, J., Bliedtner, M., Strobel, P., Schumacher, J., Bazarradnaa, E., and Zech, R.: Leaf wax n-alkane patterns and compound-specific δ13C of plants and topsoils from semi-arid and arid Mongolia, Biogeosciences, 17, 567–580, https://doi.org/10.5194/bg-17-567-2020, 2020.

54. Sun, B., Li, C., Cordovil, C., Jia, K., Zhang, S., de Varennes, A., and Pereira, L. S.: Variability of water quality in Wuliangsuhai Lake receiving drainage water from Hetao Irrigation system in Yellow River Basin, China, Fresenius Environ. Bull., 22, 1666–1676, 2013.

55. Sun, D., He, Y., Wu, J., Liu, W., and Sun, Y.: Hydrological and ecological controls on autochthonous carbonate deposition in lake systems: A case study from Lake Wuliangsu and the global perspective, Geophys. Res. Lett., 46, 6583–6593, https://doi.org/10.1029/2019GL082224, 2019.

56. Sun H., Yu, R., Liu, X., Cao, Z., Li, X., Zhang, Z., Wang, J., Zhuang, S., Ge, Z., Zhang, L., Sun, L., Lorke, A., Yang, J., Lu, C., and Lu, X.: Drivers of spatial and seasonal variations of CO_2 and CH_4 fluxes at the sediment water interface in a shallow eutrophic lake, Water Res., 222, 118916, https://doi.org/10.1016/j.watres.2022.118916, 2022.

57. Sun, H., He, J., Lü, C., Gao, X., Fan, Q., and Xue, H.: Nitrogen pollution and spatial distribution pattern of Wuliangsuhai Lake, Geographical Res., 25, 1003–1012, https://doi.org/10.11821/yj2006060007, 2006.

58. Tian, W. 2020. Simulation and Analysis on the euphotic zone and primary production of phytoplankton in Wuliangsu. Ph.D thesis Inner Mongolia Agricultural University, China (in Chinese). https://doi.org/10.27229/d.cnki.gnmnu.2020.000051

59. Tian, Z., Li, C., Shi, X., Li, W., and Zhao, S., 2011. Spatial Distribution and Storage Characteristic of Organic Carbon in Sediments of Wuliangsuhai Lake. Water Saving Irrigation, 03, 23–25. In Chinese.

60. Van Beilen, J., Li, Z., Duetz, W., Smits, T., and Witholt, B.: Diversity of alkane hydroxylase systems in the environment,

Oil Gas Sci. Technol., 58, 427–440, https://doi.org/10.2516/ogst:2003026, 2003.

61. Verpoorter, C., Kutser, T., Seekell, D. A., and Tranvik., L. J.: A global inventory of lakes based on high-resolution satellite imagery, Geophys. Res. Lett., 41, 6396–6402, https://doi.org/10.1002/2014GL060641, 2014.
62. Wang, B., Yang, J., Jiang, H., Zhang, G., and Dong, H.: Chemical composition of *n*-alkanes and microbially mediated *n*-alkane degradation potential differ in the sediments of Qinghai-Tibetan lakes with different salinity, Chem. Geol., 524, 37–48, https://doi.org/10.1016/j. chemgeo. 2019. 05. 038, 2019.
63. Wu, Y., Chao, L., Li, C., and Shi, X.: The spatial distribution characteristics of nutrient elements and heavy metals in surface sediments of lake Wuliangsuhai, J. Arid Land Resources and Environ., 4, 143–148, https://doi.org/10.13448/j.cnki.jalre.2011.04.014, 2011.
64. Wu, J., Ma, L., Yu, H., Zeng, H., Liu, W., and Abuduwaili, J.: Sediment geochemical records of environmental change in Lake Wuliangsu, Yellow River Basin, north China, J. Paleolimn., 50, 245–255, https://doi.org/10.1007/s10933-013-9718-6, 2013.
65. Wu, W., Ruan, J., Ding, S., Zhao, L., Xu, Y., Yang, H., Ding, W., and Pei, Y.: Source and distribution of glycerol dialkyl glycerol tetraethers along lower Yellow River-estuary-coast transect, Mar. Chem., 158, 17–26, https://doi.org/10.1016/j.marchem.2013.11.006, 2014.
66. Yang Z. 2009. The purification abilities of emergent plants (Phragmites) for eutrophic elements in Lake Wuliangsuhai (In Chinese). Master thesis Inner Mongolia Agricultural University
67. Yang, H., Pancost, R. D., Dang, X., Zhou, X., Evershed R. P., Xiao G., Tang C., Li, G., Guo, Z., and Xie, S.: Correlations between microbial tetraether lipids and environmental variables in Chinese soils: Optimizing the paleo-reconstructions in semi-arid and arid regions, Geochim. Cosmochim. Acta., 126, 49–69, https://doi.org/10.1016/j.gca.2013.10.041, 2014.
68. Yang, Y., Weng, B., Bi, W., Xu, T., Yan, D., and Ma, J.: Climate Change Impacts on Drought-Flood Abrupt Alternation and Water Quality in the Hetao Area, China, Water, 11, 652, https://doi.org/10.3390/w11040652, 2019.
69. Yu, R., Liu, Y., Xu, Y., and Li, C.: The impacts of human activities on the Wuliangsuhai wetland environment, J. Lake Sci., 19, 465–472, https://doi:10.18307/2007.0416, 2007.
70. Yu, X., Lü, X., Meyers, P., and Huang. X.: Comparison of molecular distributions and carbon and hydrogen isotope compositions of *n*-alkanes from aquatic plants in shallow freshwater lakes along the middle and lower reaches of the Yangtze River, China, Org. Geochem., 158, 104270, https://doi.org/10.1016/j.orggeochem.2021.104270, 2021.
71. Zhang, F., Shi, X., Zhao, S., Hao, R., and Zhai, J.: Equilibrium analysis of dissolved oxygen in Lake Wuliangsuhai during ice-covered period, J. Lake Sci., 34, 1570–1583, https://doi.org/10.18307/2022.0513, 2022.
72. Zhang, W., 2017. Using remote sensing technology to extract phragmites australis and estimate aboveground biomass in Wuliangsu. Master thesis Inner Mongolia University, China (in Chinese).
73. Zhao, Y., Yang, Z., Xia, X., and Wang, F.: A shallow lake remediation regime with *Phragmites australis*: Incorporating

https://doi.org/10.5194/bg-2023-134
Preprint. Discussion started: 17 August 2023

755 nutrients removal and water evapotranspiration, Water Res., 46, 5635–5644, https://doi.org/10.1016/j.watres.2012.07.053, 2012.

74. Zhou, L., and Zhou, G., Measurement and modelling of evapotranspiration over a reed (*Phragmites australis*) marsh in Northeast China, J. Hydrol., 372, 41–47, https://doi.org/10.1016/j.jhydrol.2009.03.033, 2009.

75. Zhu, Z., Song, S., Yan, Y., Li, P., Jeelani, N., Wang, P., An, S., and Leng. X.: Combined effects of light reduction and 760 ammonia nitrogen enrichment on the submerged macrophyte Vallisneria natans, Mar. Freshw. Res., 69, 764–770, https://doi.org/10.1071/mf17146, 2018.